# Unidirectional waves in discrete plasmonic waveguides

Vadim A. Markel[0000−0002−9748−6865]

**Abstract** Surface plasmon polaritons (SPPs) in chains of plasmonic nanoparticles have attracted significant attention due to potential applications in spectroscopy, sensing, and subwavelength manipulation of electromagnetic energy. On aspect of such waveguides that received relatively little attention is directionality. Here we explore waveguides that are not invariant under the reflection of direction. We show that, although the dispersion relations in such waveguides are still symmetric as is required by the electromagnetic reciprocity, a localized excitation applied to a central part of the chain can selectively couple to the SPPs propagating in only one of the two possible directions.

## 1 Introduction

Linear periodic chains of metal nanoparticles have attracted significant attention in the past twenty years or so with envisaged applications in spectroscopy and sensing [1–4] as well as in waveguiding and information transfer [5–8]. In our previous work, we investigated the electromagnetic properties of simple linear plasmonic chains using the point dipole approximation [9–12]. Theories accounting for higher-order multipole interactions have also been developed [13–15]. Topological properties of Bloch modes in chains with a more complicated geometry were studied in [16, 17]. Additional references can be found in the review articles [18, 19].

One aspect of plasmonic chains that received little attention so far is directionality. The radiation pattern of an electrically-small antenna is symmetric with respect to the coordinate inversion $\mathbf{r} \to -\mathbf{r}$. If such an antenna illuminates a small central segment of a chain that is invariant under the same transformation, the electromagnetic excitation in the form of a surface plasmon polariton (SPP) will travel in both directions with the same amplitude. However, if we give the chain a sense of direction,

Unversity of Pennsylvania, e-mail: vmarkel@upenn.edu

the inversion symmetry of the system "antenna+chain" would be broken. In this case, it is possible to engineer the source antenna so that it would send the SPP in one direction only. The direction can be switched by tuning the phase relations of the elementary dipoles comprising the antenna. When placed in free space, the source antenna of this type would radiate as a single dipole (in the radiation zone). However, when placed in a close vicinity of a directional chain, it will send the SPP in only one of the two possible directions, depending on its internal phase relations. Intuition may suggests that such direction-selective coupling is possible only if non-reciprocal materials are used in the chain. However, we will show that non-reciprocity is not required. This is so because the operator of dipole sum, which plays a fundamental role in the theory of discrete waveguides, is not generally symmetric, even if all the materials involved are reciprocal.

This chapter contains the general theory of directional discrete waveguides in the framework of the point dipole approximation and a numerical example demonstrating the feasibility of direction-selective coupling. While under some conditions the dipole approximation may not be accurate, the basic observation that the dipole sum in chains with a sense of direction is not symmetric is not expected to change if we account for the higher multipoles, or use a more general method for solving the electromagnetic problem. In Section 2 we describe the geometry of a discrete structured chain. Section 3 introduces the coupled-dipole equation and the dipole sum. In Section 4 we derive the dispersion equation that is specific to metal particles with the Drude dielectric function. In Section 5 we discuss some algebraic properties of the dispersion equation, which will prove useful for understanding the direction-selective coupling. In Section 7 we provide a simple example of a directional chain and demonstrate that direction-selective coupling is possible. Section 8 contains a discussion and further examples. Gaussian system of base dimensions and the corresponding form of electromagnetic equations are used throughout.

## 2 Waveguide geometry

Consider a linear discrete waveguide consisting of periodically-arranged, electrically-small particles of the same permittivity $\epsilon(\omega)$ embedded in a host medium with the constant dielectric permittivity $\epsilon_h \geq 1$ where $\epsilon_h = 1$ corresponds to vacuum and $\omega$ is the frequency. We work in the dipole approximation, so that the only relevant parameters of a particle are its location and the dipole polarizability tensor $\hat{\alpha}(\omega)$. We will use the model of metal ellipsoids to obtain physically-accessible values of $\hat{\alpha}(\omega)$ while making sure that the dipole approximation is still valid. In this case, the location coincides with the ellipsoid center and $\hat{\alpha}(\omega)$ can be expressed analytically in terms of the ellipsoid semi-axes and $\epsilon(\omega)$. While the ellipsoids comprising the waveguide can have different shapes and orientations, we assume that the material from which the particles are made is the same; otherwise, theory becomes too complicated.

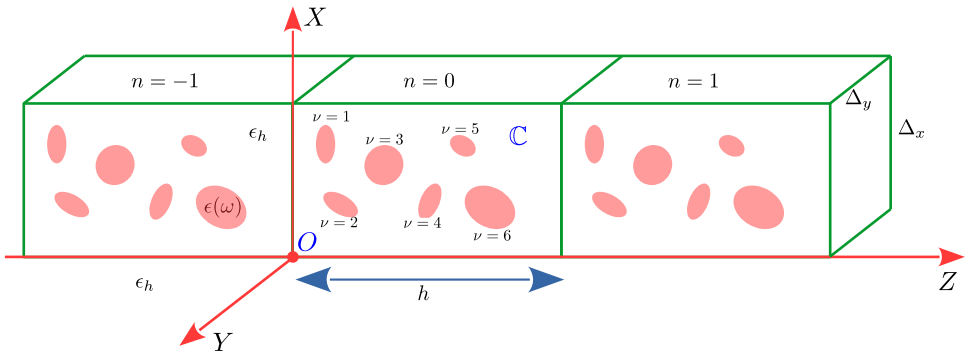


**Fig. 1** Schematic illustration of a discrete waveguide with $p = 6$ particles per cell. Three unit cells are shown including the reference cell $\mathbb{C}$ with the index $n = 0$.

Geometry of a discrete waveguide is illustrated in Fig. 1. The system is periodic in the $Z$ direction with the lattice step $h$, and we label the unit cells by $n = 0, \pm1, \pm2, ....$ Each cell contains $p > 0$ particles labeled by $\nu = 1, 2, ..., p$. We introduce the composite index $(n\nu)$ to label the particles. The locations and dipole moments of all particles are denoted by $\mathbf{r}_{n\nu} = (x_\nu, y_\nu, z_{n\nu})$ and $\mathbf{d}_{n\nu}$. Here $x_\nu$ and $y_\nu$ are independent of $n$ due to periodicity and

$$z_{n+1,\nu} = z_{n\nu} + h \, . \tag{1}$$

As the polarizabilities are also periodic, we write $\hat{\alpha}_\nu(\omega)$ for $\nu$-th article in an arbitrary cell. The set of points $\mathbf{r}_{0\nu}$ together with the polarizabilities $\hat{\alpha}_\nu$ define the reference unit cell $\mathbb{C}$. Thus, the waveguide consists of three-dimensional rectangular cells periodically repeated in the $Z$-direction; however, there is no periodicity in $X$ or $Y$. Note that the transverse dimensions of a unit cell $\Delta_x$ and $\Delta_y$ are ambiguous and do not enter any equations; we have introduced these quantities in the figure only for visual convenience.

## 3 Coupled dipole equation and the dipole sum

The frequency-domain coupled dipole equations in the discrete waveguide have the form

$$\hat{\chi}_\nu(\omega)\, \mathbf{d}_{n\nu} = \mathbf{e}_{n\nu} + \sum_{\substack{m\mu \\ (m\mu)\neq(n\nu)}} \hat{G}(\mathbf{r}_{n\nu}, \mathbf{r}_{m\mu};\, \omega)\, \mathbf{d}_{m\mu} \, , \tag{2}$$

where

$$\hat{\chi}_\nu(\omega) = \hat{\alpha}_\nu^{-1}(\omega) \tag{3}$$

is the inverse polarizability tensor, $\mathbf{d}_{n\nu}$ are the dipole moments, $\mathbf{e}_{n\nu}$ are the external fields (e.g., generated by a source antenna), $\omega$ is the working frequency, and $\hat{G}(\mathbf{r}, \mathbf{r}'; \omega)$ is the free-space Green's tensor for the electric field. We have tacitly assumed that $\hat{\alpha}_\nu(\omega)$ are invertible, which is the case for ellipsoids with any realistic dielectric function $\epsilon(\omega) \neq \epsilon_h$. The condition $(n\nu) \neq (m\mu)$ ensures that the electric field at the particle $(n\nu)$ is the sum of the external field $\mathbf{e}_{n\nu}$ and the fields generated by all other particles excluding the particle $(n\nu)$ itself. Additional details pertaining to the form of the coupled dipole equation (2), alternative forms of this equation, and accounting for the radiative correction to the quasi-static polarizability can be found in [20].

The expression for $\hat{G}$ applicable to free space is given in the Appendix. What is important for us now is that the Green's tensor satisfies the following symmetry properties:

$$\hat{G}(\mathbf{r}, \mathbf{r}'; \omega) = \hat{G}^T(\mathbf{r}', \mathbf{r}; \omega) \,, \tag{4a}$$

$$\hat{G}(\mathbf{r}, \mathbf{r}'; \omega) = \hat{G}(\mathbf{r} + s\hat{\mathbf{z}}, \mathbf{r}' + s\hat{\mathbf{z}}; \omega) \,. \tag{4b}$$

Here the superscript $T$ denotes matrix transposition and $s$ is an arbitrary real scalar (translation along the $Z$ axis). The first equation above is Lorentz reciprocity and the second is a consequence of the translational invariance of the waveguide. If the waveguide is embedded in an infinite homogeneous space, as we assume here, the Green's tensor possesses even stronger symmetries. We then have, additionally, $\hat{G}(\mathbf{r}, \mathbf{r}'; \omega) = \hat{G}^T(\mathbf{r}, \mathbf{r}'; \omega)$ and $\hat{G}(\mathbf{r}, \mathbf{r}'; \omega) = \hat{G}(\mathbf{r} + \mathbf{s}, \mathbf{r}' + \mathbf{s}; \omega)$, where $\mathbf{s}$ is an arbitrary translation vector. However, if the waveguide is placed in an external cladding, the latter properties may be lost while the properties in (4) would survive. Therefore, the theoretical results presented below are generalizable to the case of an external cladding as they rely only on (4) and not on any of the stronger symmetries.

To find guided waves, we set external fields $\mathbf{e}_{n\nu}$ to zero and seek Bloch-periodic solutions to (2) of the form

$$\mathbf{d}_{n\nu} = \mathbf{d}_\nu \, e^{\mathrm{i}\,(qh)n} \,. \tag{5}$$

Upon substituting this ansatz into (2), we obtain the equation

$$\hat{\chi}_\nu(\omega)\mathbf{d}_\nu = \sum_{\substack{m\mu \\ (m\mu)\neq(n\nu)}} \hat{G}(\mathbf{r}_{n\nu}, \mathbf{r}_{m\mu}; \omega) \, e^{\mathrm{i}\,(qh)(m-n)} \, \mathbf{d}_\mu \,. \tag{6}$$

Since summation in (6) is carried out over all integer $m$, the result does not depend on $n$ and we can set $n = 0$ in the right-hand side of (6). Using this observation, we can re-write (6) as

$$\hat{\chi}_\nu(\omega) \, \mathbf{d}_\nu = \sum_{\mu=1}^{p} \hat{S}_{\nu\mu}(\omega, q) \, \mathbf{d}_\mu \,, \tag{7}$$

where

$$\hat{S}_{\nu\mu}(\omega, q) := \sum_{\substack{m=-\infty \\ (m\mu)\neq(0\nu)}}^{\infty} \hat{G}(\mathbf{r}_{0\nu}, \mathbf{r}_{m\mu};\, \omega)\, e^{\mathrm{i}\,(qh)m} \tag{8}$$

is known as the dipole sum. Here $1 \leq \nu, \mu \leq p$. Note also that $\mathbf{r}_{0\nu}$ are in the reference cell $\mathbb{C}$.

Most previous investigations of discrete plasmonic waveguides were restricted to simple periodic 1D chains or 2D lattices where all particles are equivalent [18], although more complicated geometries have also been considered [16, 17]. In the case of simple periodic 1D chains, the dipole sum is reduced to a $3\times3$ tensor $\hat{S}(\omega, q)$, which is diagonal in the reference frame of Fig. 1. It is straightforward to show that $\hat{S}(\omega, q) = \hat{S}^T(\omega, q)$ and $\hat{S}(\omega, -q) = \hat{S}(\omega, q)$. These symmetry relations are special cases of the more general relation

$$\hat{S}_{\nu\mu}(\omega, -q) = \hat{S}^T_{\mu\nu}(\omega, q)\ , \tag{9}$$

which is applicable to structured chains. And while it is possible, under some additional conditions, to have $\hat{S}_{\nu\mu}(\omega, -q) = \hat{S}_{\nu\mu}(\omega, q)$, the latter relation does not always hold. This observation is the main difference between simple and structured chains, and it will be exploited below to find localized excitation schemes that excite only the SPPs propagating in a given direction along the chain. We refer to this phenomenon as to the direction-selective coupling and to the resulting SPPs as uni-directional.

We can prove (9) by starting from the definition (8) and following the chain of equalities

$$\begin{aligned}
\hat{S}_{\nu\mu}(\omega, -q) &= \sum_{\substack{m=-\infty \\ (0\nu)\neq(m\mu)}}^{\infty} \hat{G}(\mathbf{r}_{0\nu}, \mathbf{r}_{m\mu};\, \omega)\, e^{-\mathrm{i}\,(qh)m} \\
&= \sum_{\substack{m=-\infty \\ (0\nu)\neq(-m\mu)}}^{\infty} \hat{G}(\mathbf{r}_{0\nu}, \mathbf{r}_{-m\mu};\, \omega)\, e^{\mathrm{i}\,(qh)m} \\
&= \sum_{\substack{m=-\infty \\ (0\nu)\neq(m\mu)}}^{\infty} \hat{G}(\mathbf{r}_{m\nu}, \mathbf{r}_{0\mu};\, \omega)\, e^{\mathrm{i}\,(qh)m} \\
&= \sum_{\substack{m=-\infty \\ (0\nu)\neq(m\mu)}}^{\infty} \hat{G}^T(\mathbf{r}_{0\mu}, \mathbf{r}_{m\nu};\, \omega)\, e^{\mathrm{i}\,(qh)m} \\
&= \hat{S}^T_{\mu\nu}(\omega, q)\ .
\end{aligned} \tag{10}$$

To derive the third expression above, we have used translational invariance of $\hat{G}$, Eq. (4b). In the fourth expression, we have used Lorentz reciprocity, Eq. (4a).

## 4 Inverse polarizability and dispersion equation

Equation (6) is a set of linear homogeneous equations with a $3p \times 3p$ matrix $\mathtt{M}(\omega, q)$ (we denote $3p$-dimensional quantities such as matrices and vectors by a straight typewriter-style letters like $\mathtt{M}$ or $\mathtt{f}$). Correspondingly, the dispersion equation has the general form $\det[\mathtt{M}(\omega, q)] = 0$. The set of complex pairs $(\omega, q)$ that satisfy this equation is a rather complicated 4-dimensional algebraic variety. To simplify the problem, we can apply various physically-motivated restrictions. For example, we will consider below only real frequencies $\omega$. We will also use a more specific expression for $\hat{\chi}_\nu(\omega)$, which will allow us to disentangle the material and geometric properties of the chain in the expression for $\mathtt{M}(\omega, q)$.

First, to ensure energy conservation and mathematical stability of numerical results, we account for the first nonvanishing radiative correction to the quasi-static polarizability of an ellipsoid [20] by writing

$$\hat{\chi}(\omega) = \hat{\alpha}_{\rm qs}^{-1}(\omega) - \mathrm{i}\,\frac{2k^3}{3}\hat{I}\,, \quad k = \sqrt{\epsilon_h}\,\frac{\omega}{c}\,. \tag{11}$$

Here $\hat{\alpha}_{\rm qs}(\omega)$ is the quasi-static polarizability, $\hat{I}$ is the identity tensor, and $k$ is the wave number in the host medium. In the case of ellipsoids, the quasi-static probability can be conveniently written as

$$\hat{\alpha}_{\rm qs}(\omega) = \frac{\epsilon_h v}{4\pi}\sum_{j=1}^{3}\frac{\hat{\mathbf{u}}_j \otimes \hat{\mathbf{u}}_j}{\epsilon_h/[\epsilon(\omega)-\epsilon_h]+\varkappa_j}\,, \tag{12}$$

where $\hat{\mathbf{u}}_j$ are three mutually-orthogonal unit vectors, which define the principal axes of the ellipsoid, and $\varkappa_j$ are the corresponding depolarization factors ($\varkappa_1+\varkappa_2+\varkappa_3 = 1$). The ellipsoid volume $v$ is given in terms of the three semi-axes $a_j$ by

$$v = \frac{4\pi}{3}a_1 a_2 a_3\,, \tag{13}$$

and the depolarization factors $\varkappa_j$ can be expressed as functions of the two independent ratios $a_1/a_2$ and $a_1/a_3$. Now we can easily invert (12) and obtain for a generic ellipsoid

$$\hat{\chi}(\omega) = \frac{4\pi}{\epsilon_h v}\left[\frac{\epsilon_h}{\epsilon(\omega)-\epsilon_h}\,\hat{I} + \sum_{j=1}^{3}\varkappa_j\,\hat{\mathbf{u}}_j \otimes \hat{\mathbf{u}}_j\right] - \mathrm{i}\,\frac{2k^3}{3}\,\hat{I}\,. \tag{14}$$

It is notable that the scalar factor

$$s(\omega) := \frac{\epsilon_h}{\epsilon(\omega)-\epsilon_h} \tag{15}$$

is independent of the ellipsoid shape while the tensor

$$\hat{K} := \sum_{j=1}^{3} \varkappa_j \, \hat{\mathbf{u}}_j \otimes \hat{\mathbf{u}}_j \tag{16}$$

is independent of the material properties. The function $s(\omega)$ defined in (15) is known in the theory of composites as the Bergman-Milton spectral parameter. Further, the radiative correction depends only on the frequency. We have therefore disentangled the geometric and material properties of an ellipsoid. Returning to the problem at hand, we can write for the $\nu$-th ellipsoid

$$\hat{\chi}_\nu(\omega) = \frac{1}{\beta_\nu} \left[ s(\omega) \, \hat{I} \, + \, \hat{K}_\nu \right] \, - \, \mathrm{i} \, \frac{2k^3}{3} \, \hat{I} \, , \tag{17}$$

where

$$\beta_\nu := \frac{\epsilon_h v_\nu}{4\pi} \, . \tag{18}$$

Equation (17) is the expression we sought. Here only the geometric tensor $\hat{K}_\nu$ and the volume-related coefficient $\beta_\nu$ depend on the ellipsoid index. Note that all tensors $\hat{K}_\nu$ are symmetric, so that $\hat{K}_\nu = \hat{K}_\nu^T$.

Although equation (17) applies to any material of the ellipsoids, we will specialize below to the case when this material is a Drude metal with the permittivity

$$\epsilon(\omega) = \epsilon_0 - \frac{\omega_p^2}{\omega(\omega + \mathrm{i}\,\gamma)} \, , \tag{19}$$

where $\omega_p$ is the plasma frequency and $\gamma$ is the relaxation constant. We then have

$$s(\omega) = \epsilon_h \, \frac{\omega(\omega + \mathrm{i}\,\gamma)}{(\epsilon_0 - \epsilon_h)\omega(\omega + \mathrm{i}\,\gamma) - \omega_p^2} \, . \tag{20}$$

This expression becomes particularly simple in the case $\epsilon_0 = \epsilon_h$.

We now return to (7) and use the functional form (17) of $\hat{\chi}_\nu(\omega)$. This results in the equation

$$s(\omega) \, \mathbf{d}_\nu = \beta_\nu \left[ \sum_{\mu=1}^{p} \hat{S}_{\nu\mu}(\omega, q) \, \mathbf{d}_\mu \, + \, \mathrm{i} \, \frac{2k^3}{3} \mathbf{d}_\nu \right] \, - \, \hat{K}_\nu \, \mathbf{d}_\nu \, . \tag{21}$$

We need to find points in the two-dimensional region

$$\mathbb{D} := \left\{ -\frac{\pi}{h} \le q \le \frac{\pi}{h}; \; \omega > 0 \right\} \tag{22}$$

of the $(q, \omega)$-plane for which (21) has non-trivial solutions. Of course, this is possible only if $\gamma = 0$ in the Drude formula and then only for $q > k$ (above the light line). To find the dispersion curves numerically, we will set $\gamma = 0$ in the expression for $s(\omega)$ (20), so that

$$s(\omega) \xrightarrow[\gamma=0]{} s_0(\omega) := \frac{\epsilon_h\,\omega^2}{(\epsilon_0-\epsilon_h)\omega^2-\omega_p^2}\,. \tag{23}$$

However, when simulating propagation due to an external excitation (e.g., by an antenna), we will include finite losses in the model.

## 5 Algebraic considerations

For each pair of indexes $(\nu,\mu)$, the tensor $\hat{S}_{\nu\mu}(\omega,q)$ is a $3\times3$ matrix. We can arrange these matrices into a $3p\times 3p$ matrix $\mathtt{S}(\omega,q)$ as shown below:

$$\mathtt{S}(\omega,q)=\begin{bmatrix}\hat{S}_{11}(\omega,q) & \hat{S}_{12}(\omega,q) & \ldots & \hat{S}_{1p}(\omega,q)\\ \hat{S}_{21}(\omega,q) & \hat{S}_{22}(\omega,q) & \ldots & \hat{S}_{2p}(\omega,q)\\ \ldots & \ldots & \ldots & \ldots\\ \ldots & \ldots & \ldots & \ldots\\ \hat{S}_{p1}(\omega,q) & \hat{S}_{p2}(\omega,q) & \ldots & \hat{S}_{pp}(\omega,q)\end{bmatrix}. \tag{24}$$

We denote matrices of the size $3p\times 3p$ by straight, typewriter-style letters such as $\mathtt{S}$. We can use (4) to show that

$$\mathtt{S}(\omega,-q)=\mathtt{S}^T(\omega,q)\,. \tag{25}$$

We also introduce two block-diagonal matrices

$$\mathtt{B}=\begin{bmatrix}\beta_1\hat{I} & 0 & \ldots & 0\\ 0 & \beta_2\hat{I} & \ldots & 0\\ \ldots & \ldots & \ldots & \ldots\\ \ldots & \ldots & \ldots & \ldots\\ 0 & 0 & \ldots & \beta_p\hat{I}\end{bmatrix},\qquad \mathtt{K}=\begin{bmatrix}\hat{K}_1 & 0 & \ldots & 0\\ 0 & \hat{K}_2 & \ldots & 0\\ \ldots & \ldots & \ldots & \ldots\\ \ldots & \ldots & \ldots & \ldots\\ 0 & 0 & \ldots & \hat{K}_p\end{bmatrix}. \tag{26}$$

Then Eq. (21) takes the following form:

$$s(\omega)\,\mathtt{d}=\mathtt{W}(\omega,q)\,\mathtt{d}\,, \tag{27}$$

where

$$\mathtt{W}(\omega,q)=\mathtt{B}\left[\,\mathtt{S}(\omega,q)+\mathrm{i}\,\frac{2k^3}{3}\mathtt{I}\,\right]-\mathtt{K} \tag{28}$$

and $\mathtt{d}$ is a column-vector of dipole moments $\mathbf{d}_\nu$ of the length $3p$:

$$\mathtt{d}=\begin{bmatrix}\mathbf{d}_1 & \mathbf{d}_2 & \ldots & \ldots & \mathbf{d}_p\end{bmatrix}^T\,. \tag{29}$$

Equation (27) has nontrivial solutions if and only if one of the eigenvalues of $\mathtt{W}(\omega,q)$ is equal to $s(\omega)$.

### 5.1 Ellipsoids of equal volume

Let us first analyze the relatively simple case when $\mathtt{B}$ is proportional to the identity matrix, $\mathtt{B} = \beta\mathtt{I}$. This happens if all ellipsoids are of the same volume (but not necessarily of the same shape and orientation). Then the symmetry property (25) of $\mathtt{S}(\omega, q)$ is inherited by $\mathtt{W}(\omega, q)$. Indeed, we have in the special case considered

$$\mathtt{W}(\omega, q) = \beta \left[ \mathtt{S}(\omega, q) + \mathrm{i}\,\frac{2k^3}{3}\mathtt{I} \right] - \mathtt{K}\,. \tag{30}$$

Here $\mathtt{I}$ is the $3p \times 3p$ identity matrix. Since $\mathtt{K}$ is symmetric and independent of $q$, we have

$$\mathtt{W}(\omega, -q) = \mathtt{W}^T(\omega, q) \quad (\text{if } \beta_\nu = \beta = \text{const})\,. \tag{31}$$

It immediately follows that $\mathtt{W}(\omega, q)$ and $\mathtt{W}(\omega, -q)$ have the same eigenvalues. Therefore, if a point $(\omega, q)$ is on the dispersion curve, then $(\omega, -q)$ is also on the dispersion curve (because $s(\omega)$ is independent of $q$). We thus have proved the following theorem:

**Theorem 1** (Eigenvalues of $\mathtt{W}(\omega, q)$ for ellipsoids of fixed volume)**.** For structured chains made of general ellipsoids of equal volume, the following statements are true:

(i) $\mathtt{W}(\omega, q)$ and $\mathtt{W}(\omega, -q)$ share the same set of eigenvalues $\lambda_i(\omega, q)$. Therefore, the eigenvalues are even functions of $q$, $\lambda_i(\omega, -q) = \lambda_i(\omega, q)$.

(ii) The dispersion curves $q = q(\omega)$ are symmetric with respect to the line $q = 0$.

Moreover, it is clear that, if $\mathtt{f}(\omega, q)$ and $\mathtt{f}(\omega, -q)$ are the right eigenvectors of $\mathtt{W}(\omega, q)$ and $\mathtt{W}(\omega, -q)$, respectively, with the same eigenvalue $\lambda(\omega, q)$, then $\mathtt{f}(\omega, -q)$ is a left eigenvector of $\mathtt{W}(\omega, q)$ and $\mathtt{f}(\omega, q)$ is a left eigenvector of $\mathtt{W}(\omega, -q)$. Indeed, start from the definitions

$$\begin{aligned} \mathtt{W}(\omega,\ \ q)\ \mathtt{f}(\omega,\ \ q) &= \lambda(\omega, q)\ \mathtt{f}(\omega,\ \ q)\,, \\ \mathtt{W}(\omega, -q)\ \mathtt{f}(\omega, -q) &= \lambda(\omega, q)\ \mathtt{f}(\omega, -q)\,. \end{aligned} \tag{32a}$$

Transposing the above equations and using (31), we obtain

$$\begin{aligned} \mathtt{f}^T(\omega,\ \ q)\ \mathtt{W}(\omega, -q) &= \lambda(\omega, q)\ \mathtt{f}^T(\omega,\ \ q)\,, \\ \mathtt{f}^T(\omega, -q)\ \mathtt{W}(\omega,\ \ q) &= \lambda(\omega, q)\ \mathtt{f}^T(\omega, -q)\,, \end{aligned} \tag{32b}$$

which proves the above statement.

**Theorem 2** (Eigenvectors of $\mathtt{W}(\omega, q)$ for ellipsoids of fixed volume)**.** Assume that $\mathtt{W}(\omega, q)$ has $3p$ distinct eigenvalues $\lambda_i(\omega, q)$ corresponding to the eigenvectors $\mathtt{f}_i(\omega, q), i = 1, 2, ..., 3p$. Then $\mathtt{W}(\omega, -q)$ has $3p$ eigenvectors $\mathtt{f}_i(\omega, -q)$ corresponding to the same distinct eigenvalues and the two sets of eigenvectors are mutually dual bases so that

$$\mathtt{f}_j^T(\omega, -q)\, \mathtt{f}_i(\omega, q) = Z_i(\omega, q)\, \delta_{ji}$$

with $Z_i(\omega, q) \neq 0$ and $Z_i(\omega, -q) = Z_i(\omega, q)$.

Note that there is no complex conjugation in the orthogonality relation of Theorem 2. We can still normalize the eigenvectors by the conventional condition

$$\mathtt{f}_i^\dagger(\omega, q)\, \mathtt{f}_i(\omega, q) = 1\ . \tag{33}$$

Here † denotes Hermitian conjugation (transposition and entry-wise complex conjugation).

*Proof.* The first statement of Theorem 2 is obvious. Eigenvectors of any non-degenerate matrix form a basis, and $\mathtt{W}(\omega, q)$ and $\mathtt{W}(\omega, -q)$ share the same set of distinct eigenvalues. To show that the two bases are dual, we can consider the matrix element

$$\mathtt{f}_j^T(\omega, -q)\, \mathtt{W}(\omega, q)\, \mathtt{f}_i(\omega, q) \tag{34}$$

and use the relations (32). Acting with $\mathtt{W}(\omega, q)$ to the left and to the right, we obtain the equality

$$\lambda_i(\omega, q)\ \mathtt{f}_j^T(\omega, -q)\, \mathtt{f}_i(\omega, q) = \lambda_j(\omega, q)\ \mathtt{f}_j^T(\omega, -q)\, \mathtt{f}_i(\omega, q)\ . \tag{35}$$

If $j \neq i$, the above equality implies that $\mathtt{f}_j^T(\omega, -q)\, \mathtt{f}_i(\omega, q) = 0$. This proves mutual orthogonality of the bases. It remains to show that $Z_i(\omega, q) \neq 0$. Assume that $Z_i(\omega, q) = 0$ for some $i$. We know that $\mathtt{f}_j^T(\omega, -q)\, \mathtt{f}_i(\omega, q) = 0$ for all $j \neq i$. Therefore, the set of $\mathtt{f}_j(\omega, -q)$ with $j \neq i$ forms the orthogonal complement to $\mathtt{f}_i(\omega, q)$. If, in addition, $\mathtt{f}_i(\omega, -q)$ has zero projection onto $\mathtt{f}_i(\omega, q)$, the set of all vectors $\mathtt{f}_j(\omega, -q)$ is the same orthogonal complement and therefore does not form a complete basis in contradiction to the assumption that $\mathtt{W}(\omega, q)$ is non-degenerate. Therefore, $Z_i(\omega, q) = 0$ is not a possibility. □

We can now write the following spectral expansion for $\mathtt{W}(\omega, q)$ (assuming it is not degenerate)

$$\mathtt{W}(\omega,q)=\sum_{i=1}^{3p}\frac{1}{Z_i(\omega,q)}\,\lambda_i(\omega,q)\,\mathtt{f}_i(\omega,q)\,\mathtt{f}_i^T(\omega,-q)\ . \tag{36}$$

**Remark 1** (Degeneracy of $\mathtt{W}(\omega,q)$)**.** If $\mathtt{W}(\omega,q)$ is degenerate but not defective (this means that its eigenvectors still form a complete basis), we can always construct dual bases of eigenvectors of $\mathtt{W}(\omega,q)$ and $\mathtt{W}(\omega,-q)$ according to the standard procedure. This case does not pose any difficulties and the statements of Theorem (2) remain true. However, $\mathtt{W}(\omega,q)$ is, in general, neither symmetric nor Hermitian, and proving non-defectiveness for matrices with no special symmetry is usually difficult. From the physical point of view, defectiveness occurs due to random degeneracy with a probability close to 0 and therefore almost never. In simulations, it is safe to ignore this possibility.

## 5.2 Ellipsoids of varying volume

It is clear on physical grounds that allowing the volume of ellipsoids to vary should not cause any new effects. In fact, the spectral properties of $\mathtt{W}(\omega,q)$ remain in this case almost the same (with a slight modification), but the proofs are more difficult because $\mathtt{B}$ is no longer proportional to the identity matrix and the symmetry relation (31) does not hold.

We start from the definition (28) where $\mathtt{B}$ is not necessarily proportional to the identity matrix, and write it in the form

$$\mathtt{W}(\omega,q)=\mathtt{B}\,\mathtt{S}(\omega,q)\ +\ \mathrm{i}\,\frac{2k^3}{3}\mathtt{B}\ -\ \mathtt{K}\,. \tag{37}$$

Next we change the sign of $q$ in the previous formula. This yields

$$\mathtt{W}(\omega,-q)=\mathtt{B}\,\mathtt{S}(\omega,-q)\ +\ \mathrm{i}\,\frac{2k^3}{3}\mathtt{B}\ -\ \mathtt{K}\,. \tag{38}$$

Using the symmetry property (25) of $\mathtt{S}(\omega,q)$, we also have

$$\mathtt{W}(\omega,-q)=\left[\mathtt{S}(\omega,q)\,\mathtt{B}\ +\ \mathrm{i}\,\frac{2k^3}{3}\mathtt{B}\ -\ \mathtt{K}\right]^T\ , \tag{39}$$

where we accounted for the symmetry of $\mathtt{B}$ and $\mathtt{K}$. Let us denote the matrix in the square brackets by $\mathtt{U}(\omega,q)$;

$$\mathtt{U}(\omega,q) := \mathtt{S}(\omega,q)\,\mathtt{B} + \mathrm{i}\,\frac{2k^3}{3}\mathtt{B} - \mathtt{K}\,. \tag{40}$$

We therefore have

$$\mathtt{W}(\omega,-q) = \mathtt{U}^T(\omega,q)\,. \tag{41}$$

The matrices $\mathtt{S}(\omega,q)$ and $\mathtt{B}$ do not generally commute. For this reason, $\mathtt{U}(\omega,q) \neq \mathtt{W}(\omega,q)$. We will however prove that $\mathtt{U}(\omega,q)$ and $\mathtt{W}(\omega,q)$ share the same eigenvalues. To this end, we will use the special properties of $\mathtt{B}$ and $\mathtt{K}$. It will then follow from (41) that $\mathtt{W}(\omega,q)$ and $\mathtt{W}(\omega,-q)$ share the same eigenvalues, even though these two matrices are not transposes of each other.

**Theorem 3** (Eigenvalues of $\mathtt{W}(\omega,q)$ for ellipsoids of variable volume)**.** Conclusions of Theorem 1 carry over to the case when the ellipsoids have variable volume.

*Proof.* We can prove Theorem 3 by noticing that $\mathtt{B}$ is diagonal and all its elements are positive and removed from zero (since the same is true for the volumes $v_\nu$). We can therefore take the square root of $\mathtt{B}$ and, moreover, this operation is numerically stable. Let $\mathtt{B} = \mathtt{D}\,\mathtt{D}$. From the same arguments as above, $\mathtt{D}$ is invertible. We can use these properties of $\mathtt{B}$ to write

$$\begin{aligned}
\mathtt{W}(\omega,q) &= \mathtt{D}\quad\left[\mathtt{D}\,\mathtt{S}(\omega,q)\,\mathtt{D} + \mathrm{i}\,\frac{2k^3}{3}\mathtt{B} - \mathtt{D}^{-1}\,\mathtt{K}\,\mathtt{D}\quad\right]\mathtt{D}^{-1}\,,\\
\mathtt{U}(\omega,q) &= \mathtt{D}^{-1}\left[\mathtt{D}\,\mathtt{S}(\omega,q)\,\mathtt{D} + \mathrm{i}\,\frac{2k^3}{3}\mathtt{B} - \mathtt{D}\quad\mathtt{K}\mathtt{D}^{-1}\right]\mathtt{D}\quad.
\end{aligned} \tag{42}$$

The key observation that we need is that $\mathtt{D}^{-1}\,\mathtt{K}\,\mathtt{D} = \mathtt{D}\,\mathtt{K}\,\mathtt{D}^{-1} = \mathtt{K}$. This is easy to verify directly. Denoting

$$\mathtt{W}_s(\omega,q) := \mathtt{D}\,\mathtt{S}(\omega,q)\,\mathtt{D} + \mathrm{i}\,\frac{2k^3}{3}\mathtt{B} - \mathtt{K}\,, \tag{43}$$

we arrive at the result

$$\begin{aligned}
\mathtt{W}(\omega,q) &= \mathtt{D}\quad\mathtt{W}_s(\omega,q)\,\mathtt{D}^{-1}\,,\\
\mathtt{U}(\omega,q) &= \mathtt{D}^{-1}\,\mathtt{W}_s(\omega,q)\,\mathtt{D}\quad.
\end{aligned} \tag{44}$$

Here $\mathtt{W}_s(\omega,q)$ is the symmetrized form of $\mathtt{W}(\omega,q)$ (compare to Eq. 37). In the case when $\mathtt{B} = \beta\mathtt{I}$, the two matrices coincide. It is now easy to see that $\mathtt{W}_s(\omega,q)$, $\mathtt{W}(\omega,q)$ and $\mathtt{U}(\omega,q)$ share the same eigenvalues. This proves Theorem 3. □

**Theorem 4** (Eigenvectors of $\mathtt{W}(\omega, q)$ for ellipsoids of variable volume)**.** Let the symmetrized matrix $\mathtt{W}_s(\omega, q)$ have $3p$ distinct eigenvalues $\lambda_i(\omega, q)$, $i = 1, 2, ..., 3p$ with the corresponding eigenvectors $\mathtt{f}_i(\omega, q)$. Then $\mathtt{D}\mathtt{f}_i(\omega, q)$ and $\mathtt{D}^{-1}\mathtt{f}_i(\omega, -q)$ are the right and left eigenvectors of $\mathtt{W}(\omega, q)$ with the same eigenvalues. These two sets of eigenvectors are mutually dual bases.

The proof is obvious since $\mathtt{W}_s(\omega, q)$ satisfies the symmetry property (31) and all conclusions of Theorem 2 hold for it verbatim. In particular, (36) holds for $\mathtt{W}_s(\omega, q)$. We can therefore use (44) to write

$$\mathtt{W}(\omega, q) = \sum_{i=1}^{3p} \frac{1}{Z_i(\omega, q)}\, \lambda_i(\omega, q)\, \mathtt{D}\, \mathtt{f}_i(\omega, q)\, \mathtt{f}_i^T(\omega, -q)\, \mathtt{D}^{-1}\,. \tag{45}$$

The statements of Theorem 4 can be verified directly by using this formula.

**Remark 2** (Normalization)**.** We assume that the vectors $\mathtt{f}_i(\omega, q)$ (for positive and negative $q$) are normalized by the conventional condition

$$\mathtt{f}_i^\dagger(\omega, q)\, \mathtt{f}_i(\omega, q) = 1\,. \tag{46}$$

Then the left and right eigenvectors of $\mathtt{W}(\omega, q)$,

$$\mathtt{g}_i(\omega, q) := \mathtt{D}\mathtt{f}_i(\omega, q)\,, \quad \mathtt{g}_i(\omega, -q) := \mathtt{D}^{-1}\mathtt{f}_i(\omega, -q)$$

are not normalized. However, the overlap coefficients appearing in (45) are the same for the normalized and not normalized bases, viz,

$$Z_i(\omega, q) = Z_i(\omega, -q) = \mathtt{f}_i^T(\omega, -q)\, \mathtt{f}_i(\omega, q) = \mathtt{g}_i^T(\omega, -q)\, \mathtt{g}_i(\omega, q)\,. \tag{47}$$

## 6 Forced oscillations

### 6.1 Response to external field

We now consider the response to an external field, e.g., produced by a source antenna. To this end, we return to the coupled-dipole equation (2) and seek the solution in the form of a Fourier integral

$$\mathbf{d}_{n\nu} = \frac{1}{2\pi}\int\limits_{-\pi/h}^{\pi/h} \tilde{\mathbf{d}}_\nu(\xi)\, e^{\mathrm{i}\,\xi h n}\,\mathrm{d}\xi\ , \quad \nu = 1,2,...,p\ . \tag{48}$$

Here $\tilde{\mathbf{d}}_\nu(\xi)$ is the Fourier coefficient to be determined. A similar decomposition can be written for the incident field:

$$\mathbf{e}_{n\nu} = \frac{1}{2\pi}\int\limits_{-\pi/h}^{\pi/h} \tilde{\mathbf{e}}_\nu(\xi)\, e^{\mathrm{i}\,\xi h n}\,\mathrm{d}\xi\ , \quad \nu = 1,2,...,p\ . \tag{49}$$

Using the $3p$-dimensional matrix notations introduced above and the expression (17) for $\hat{\chi}(\omega)$, the coupled-dipole equation (2) can be written as

$$[s(\omega)\,\mathtt{I} - \mathtt{W}(\omega,\xi)]\,\tilde{\mathtt{d}}(\xi) = \mathtt{B}\,\tilde{\mathtt{e}}(\xi)\ , \tag{50}$$

with the obvious solution

$$\tilde{\mathtt{d}}(\xi) = [s(\omega)\,\mathtt{I} - \mathtt{W}(\omega,\xi)]^{-1}\ \mathtt{B}\,\tilde{\mathtt{e}}(\xi)\ . \tag{51}$$

We then substitute this result back to the Fourier integral (48) and find the real-space solution

$$\mathtt{d}_n = \frac{1}{2\pi}\int\limits_{-\pi/h}^{\pi/h} [s(\omega)\,\mathtt{I} - \mathtt{W}(\omega,\xi)]^{-1}\ \mathtt{B}\,\tilde{\mathtt{e}}(\xi)\, e^{\mathrm{i}\,\xi h n}\,\mathrm{d}\xi\ . \tag{52}$$

In this expression, $\mathtt{d}_n$ is the $3p$-dimensional vector of dipole moments in the $n$-th cell. The correspondence to the three-dimensional vectors $\mathbf{d}_{n\nu}$, that is,

$$\mathtt{d}_n = \left[\mathbf{d}_{n1}\ \mathbf{d}_{n2}\ ...\ ...\ \mathbf{d}_{np}\right]^T\ . \tag{53}$$

Next, we use the spectral expansion (45) to write

$$[s(\omega)\,\mathtt{I} - \mathtt{W}(\omega,\xi)]^{-1} = \sum_{i=1}^{3p} Z_i(\omega,\xi)\,\frac{\mathtt{D}\,\mathtt{f}_i(\omega,\xi)\,\mathtt{f}_i^T(\omega,-\xi)\,\mathtt{D}^{-1}}{s(\omega)-\lambda_i(\omega,\xi)}\ . \tag{54}$$

Substituting this result into (52), we obtain the spectral solution to the forced oscillation problem:

$$\mathtt{d}_n = \frac{1}{2\pi}\int\limits_{-\pi/h}^{\pi/h} \mathrm{d}\xi\, e^{\mathrm{i}\,\xi h n} \sum_{i=1}^{3p} Z_i(\omega,\xi)\,\frac{\mathtt{D}\,\mathtt{f}_i(\omega,\xi)\,\mathtt{f}_i^T(\omega,-\xi)\,\mathtt{D}\,\tilde{\mathtt{e}}(\xi)}{s(\omega)-\lambda_i(\omega,\xi)}\ . \tag{55}$$

In the special case when all ellipsoids are of the same volume $v$, this expression simplifies to

$$\mathtt{d}_n = \frac{\epsilon_h v}{8\pi^2} \int_{-\pi/h}^{\pi/h} \mathrm{d}\xi \, e^{\mathrm{i}\,\xi h n} \sum_{i=1}^{3p} Z_i(\omega,\xi) \, \frac{\mathtt{f}_i(\omega,\xi)\, \mathtt{f}_i^T(\omega,-\xi)\, \tilde{\mathtt{e}}(\xi)}{s(\omega) - \lambda_i(\omega,\xi)} \,. \tag{56}$$

## 6.2 Localized excitation and the quasi-particle pole approximation

Of special interest is excitation that is localized and, ideally, restricted to the reference cell. This means that

$$\mathbf{e}_{n\nu} = \mathbf{e}_\nu \, \delta_{n0} \,. \tag{57}$$

In this case,

$$\tilde{\mathbf{e}}_\nu(\xi) = h \, \mathbf{e}_\nu \tag{58}$$

is independent of $\xi$, as can be easily verified by substitution into (49). In practice, the source antenna will illuminate all particles in the chain. However, by using directional antennas or by placing them close to the reference cell, we can minimize such effects. Mathematically, however, the approximation (58) is convenient as it allows one to compute the response due to some elementary excitations whereas more complex and realistic excitations can be considered by linear superposition.

Assuming (58) is true, we re-write (55)

$$\mathtt{d}_n = \frac{h}{2\pi} \int_{-\pi/h}^{\pi/h} \mathrm{d}\xi \, e^{\mathrm{i}\,\xi h n} \sum_{i=1}^{3p} Z_i(\omega,\xi) \, \frac{\mathtt{D}\,\mathtt{f}_i(\omega,\xi)\, \mathtt{f}_i^T(\omega,-\xi)\, \mathtt{D}\,\mathtt{e}}{s(\omega) - \lambda_i(\omega,\xi)} \,, \tag{59}$$

where $\mathtt{e}$ is the $3p$-dimensional vector whose elements are the electric fields created by the source antenna at the particles of the reference cell,

$$\mathtt{e} = \left[\mathbf{e}_1 \; \mathbf{e}_2 \; \ldots \; \ldots \; \mathbf{e}_p\right]^T \,. \tag{60}$$

Equation (59) seems to be a small modification of (55) (the dependence on $\xi$ and the overhead tilde in $\tilde{\mathtt{e}}(\xi)$ are gone; note also the extra power of $h$ in the overall coefficient), but it will allow us to make further analytical progress by applying the quasi-particle pole approximation as described below.

For each $\omega$, the dominant input to the integral (59) is given by the values of $\xi$ such that the denominator $s(\omega) - \lambda_i(\omega,\xi)$ is small. If the denominator could turn to zero, the integral would be ill-defined. However, it cannot turn to zero if there is some absorption in the particle material. The approach therefore is to compute the dispersion curves by solving the equation $s(\omega) = \lambda_i(\omega,\xi)$ with zero absorption; then evaluate the integral (59) for some small but nonzero absorption. We write

$$s(\omega) = s_0(\omega) + \mathrm{i}\,\sigma(\omega) \,, \tag{61}$$

where $\sigma(\omega) > 0$ and $s_0(\omega) = \lim_{\gamma\to 0} s(\omega)$. A particular expression for $s_0(\omega)$, which can be used conveniently in numerical simulations, is given in (23). Then the dispersion curves are obtained by finding all real-valued solutions to

$$s_0(\omega) = \lambda_i(\omega,\xi) \quad \text{(dispersion equation for } i\text{-th mode)}\,, \tag{62}$$

where $\omega > 0$ and $-\pi/h < \xi \le \pi/h$.

Not all modes may have such solutions at a given frequency $\omega$. Let us fix $\omega$ and assume for simplicity that real values of $\xi$ that satisfy (62) exist only for $i = r$ (the resonant mode). If such solutions exist for several values of $i$, a generalization is easily obtained by summation over all resonant modes. Assuming for now that a solution exists only for $i = r$, we may keep only one term in the summation of (59), viz,

$$\mathtt{d}_n = \frac{h}{2\pi}\int\limits_{-\pi/h}^{\pi/h} \mathrm{d}\xi\, e^{\mathrm{i}\,\xi h n}\, Z_r(\omega,\xi)\,\frac{\mathtt{D}\,\mathtt{f}_r(\omega,\xi)\;\mathtt{f}_r^T(\omega,-\xi)\,\mathtt{D}\,\mathtt{e}}{s(\omega)-\lambda_r(\omega,\xi)}\,. \tag{63}$$

Due to the symmetry of $\lambda_i(\omega,\xi)$, roots of (62) always come in pairs. Consider the simplest case when there are only two roots, $\xi = \pm q(\omega)$, where $q(\omega) > 0$ for definitiveness. The set of all points $(\omega, q(\omega))$ defines the dispersion relation of the chain. We can expand $\lambda_r(\omega,\xi)$ for $\xi$ near the roots $\pm q(\omega)$ as

$$\lambda_r(\omega,\xi) \approx s_0(\omega) - \sigma(\omega)\,\ell(\omega) \times \begin{cases} q(\omega)-\xi\,, & \xi \approx \;\; q(\omega) \\ q(\omega)+\xi\,, & \xi \approx -q(\omega) \end{cases}\,. \tag{64}$$

Here the factor $\sigma(\omega)$ has been introduced for convenience and $\ell(\omega)$ is a new independent coefficient. It may be computed numerically as

$$\ell(\omega) := \frac{1}{\sigma(\omega)}\,\frac{\partial\lambda_r(\omega,\xi)}{\partial\xi}\bigg|_{\xi=q(\omega)}\,. \tag{65}$$

Although we do not prove this statement here, $\lambda_i(\omega,\xi)$ are real-valued for $\xi > k$ (where the solutions to the dispersion equation exist), and therefore $\ell(\omega)$ is also real. The physical interpretation is that, below the light line, the SPPs propagate without radiative losses. However, $\ell(\omega)$ can be positive or negative. We say that dispersion is positive at $\omega$ if $\ell(\omega) > 0$ and negative otherwise.

We can now use (64) to re-write (63), approximately, as

$$\mathtt{d}_n = \frac{h\,Z_r(\omega,q(\omega))}{2\pi\,\sigma(\omega)\,\ell(\omega)} \times \int\limits_{-\infty}^{\infty}\left[\,\frac{\mathtt{d}_-(\omega)}{\xi+q(\omega)+\mathrm{i}\,/\ell(\omega)} - \frac{\mathtt{d}_+(\omega)}{\xi-q(\omega)-\mathrm{i}\,/\ell(\omega)}\,\right] e^{\mathrm{i}\,\xi h n}\,\mathrm{d}\xi\,. \tag{66}$$

In this expression,

$$\mathtt{d}_+(\omega) := \mathtt{P}_r(\omega)\,\mathtt{e}\,, \quad \mathtt{d}_-(\omega) := \mathtt{P}_r^T(\omega)\,\mathtt{e}\,, \tag{67a}$$

where

$$\mathtt{P}_r(\omega) := \mathtt{D}\,\mathtt{f}_r(\omega, q(\omega))\;\mathtt{f}_r^T(\omega, -q(\omega))\,\mathtt{D}\,. \tag{67b}$$

Note that we have expanded the integration in (66) to the real axis. It remains therefore to compute the integrals in (66). Consider first the case of positive dispersion, $\ell(\omega) > 0$. Accounting for the general condition $\sigma(\omega) > 0$, we arrive at

$$\mathtt{d}_n = \frac{h\,Z_r(\omega, q(\omega))\,e^{[\mathrm{i}\,q(\omega) - 1/\ell(\omega)]h|n|}}{\mathrm{i}\,\sigma(\omega)\,\ell(\omega)} \begin{cases} \mathtt{d}_+(\omega)\,, & n > 0 \\ \dfrac{1}{2}\,[\mathtt{d}_+(\omega) + \mathtt{d}_-(\omega)]\,, & n = 0 \\ \mathtt{d}_-(\omega)\,, & n < 0 \end{cases}. \tag{68}$$

We thus see that, for a generic point $(\omega, q(\omega))$ on the dispersion curve, the propagates to the right and left of the excitation site with the wave numbers $+q(\omega)$ and $-q(\omega)$, respectively. The coefficient $\ell(\omega)$ is the characteristic propagation distance, which describes the exponential decay of the SPPs due to Ohmic losses. The amplitudes of propagation to the right and to the left are in general not the same and given by $\mathtt{d}_+(\omega)$ and $\mathtt{d}_-(\omega)$ for positive dispersion, and vice versa for negative dispersion.

## 7 Direction-selective coupling

Here we demonstrate direction-selective coupling of SPPs to local excitation (confined to the reference cell $\mathbb{C}$). The question we are asking is whether it is possible to achieve direction-selective coupling by illuminating only the dipoles in the smallest periodic element of the cell. The latter qualifier is important. There are other means to excite SPPs propagating in a given direction only, but they require a spatially-extended source antenna with the length of many periods of the chain. For example, the smallest cell in a simple linear periodic chain consists of just one particle, and local direction-selective coupling in such chains is impossible. More generally, local direction-selective coupling is not possible in chains that are invariant under the reflection $Z \to -Z$. Indeed, if the chain has this property, the matrix $W(\omega, q)$, in addition to the fundamental relation (31), is also symmetric, so that $\mathtt{W}(\omega, q) = \mathtt{W}^T(\omega, q) = \mathtt{W}(\omega, -q)$. It is easy to see from (43) that, in this case, $\mathtt{d}_+ = \mathtt{d}_-$.

However, in a chain without the reflection symmetry, $\mathtt{W}(\omega, q)$ is not symmetric. We can exploit this property to achieve direction-selective coupling with a fairly good precision. Indeed, at a frequencies corresponding to positive dispersion, direction-selective coupling to SPPs propagating to the right of the reference cell (in the positive $Z$ direction) occurs if $\mathtt{d}_+ \neq 0$ but $\mathtt{d}_- = 0$. It can be seen from (68) that, within the precision of the quasi-particle pole approximation, the dipole moments in

the cells with $n < 0$ are in this case zero. Similarly, the SPP would propagate to the left of the reference cell if $\mathtt{d}_- \neq 0$ but $\mathtt{d}_+ = 0$. For negative dispersion, the directions are reversed.

## 7.1 Directional chain with three particles per cell

There are several simple geometries of the reference cell that we can investigate for the purpose of providing examples. Here we illustrate how the direction-selective coupling can be achieved using the simple geometry illustrated in Fig. 2. Assume that the polarization is out-of-plane (along the $Y$-axis) and the particles are identical prolate spheroids whose major axis is aligned with $Y$. Fig. 2 can be regarded as the "top view" of the waveguide. Below, we provide some analytical results for this geometry and illustrate the accuracy of the quasi-particle pole approximation.

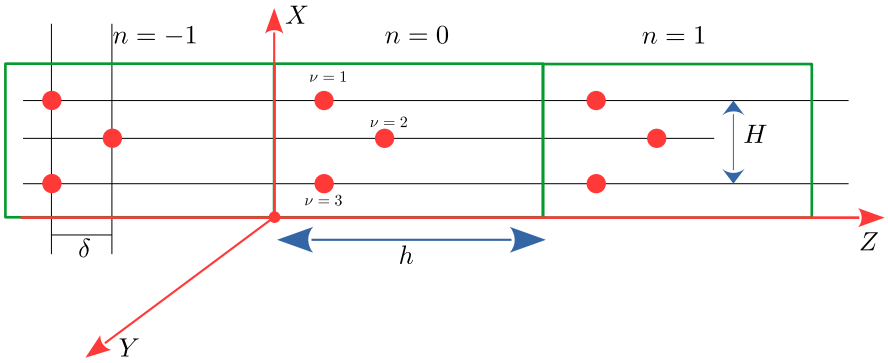


**Fig. 2** Schematic illustration of the discrete waveguide for which direction-selective coupling is possible.

Since the Cartesian components of the dipole moments along $X$ and $Z$ are zero in the considered geometry and only the $Y$-components enter the equations, the size of $\mathtt{W}$ is effectively $3\times 3$. The algebraic structure of $\mathtt{W}(\omega, q)$ is (regardless of $\omega$ and $q$)

$$\mathtt{W} = \begin{bmatrix} w_{11} & w_{12} & w_{13} \\ w_{21} & w_{22} & w_{23} \\ w_{31} & w_{32} & w_{33} \end{bmatrix} = \begin{bmatrix} a & b & c \\ d & a & d \\ c & b & a \end{bmatrix} . \tag{69}$$

Here we accounted for the symmetry relations

$$\begin{aligned} w_{11} = w_{22} = w_{33} =: a \,, \\ w_{12} = w_{32} =: b \,, \\ w_{13} = w_{31} =: c \,, \\ w_{21} = w_{23} =: d \,, \end{aligned} \tag{70}$$

which are specific to the considered geometry. It is possible to prove that, for $q > k$, $a$ and $c$ are real while $d = b^*$. Therefore, $\mathtt{W}$ is neither symmetric nor Hermitian. This fact will allow us to achieve direction-selective coupling. The matrix has three distinct eigenvalues

$$\lambda_1 = a - c \,, \quad \lambda_2 = a + \frac{c - \sqrt{c^2 + 8bd}}{2} \,, \quad \lambda_3 = a + \frac{c + \sqrt{c^2 + 8bd}}{2} \,. \tag{71}$$

It can be seen that for $q > k$ all eigenvalues are real. The dual bases of right and left eigenvectors, $\mathtt{f}_i$ and $\mathtt{g}_i$, are

$$\begin{aligned} &\mathtt{f}_1 = \begin{bmatrix} -1 & 0 & 1 \end{bmatrix}^T, \ \mathtt{f}_2 = \begin{bmatrix} 1 & \dfrac{-\sqrt{c^2 + 8bd} - c}{2b} & 1 \end{bmatrix}^T, \ \mathtt{f}_3 = \begin{bmatrix} 1 & \dfrac{\sqrt{c^2 + 8bd} - c}{2b} & 1 \end{bmatrix}^T; \\ &\mathtt{g}_1 = \begin{bmatrix} -1 & 0 & 1 \end{bmatrix}^T, \ \mathtt{g}_2 = \begin{bmatrix} 1 & \dfrac{-\sqrt{c^2 + 8bd} - c}{2d} & 1 \end{bmatrix}^T, \ \mathtt{g}_3 = \begin{bmatrix} 1 & \dfrac{\sqrt{c^2 + 8bd} - c}{2d} & 1 \end{bmatrix}^T. \end{aligned} \tag{72}$$

The orthogonality relations are, as expected, $\mathtt{f}_i^T \, \mathtt{g}_j = Z_i \, \delta_{ij}$ with

$$Z_1 = 2 \,, \quad Z_2 = Z_3 = 4 + \frac{c\left(c + \sqrt{c^2 + 8bd}\right)}{2bd} \,. \tag{73}$$

In addition, we have the following relations

$$\mathtt{f}_2^T \, \mathtt{f}_3 = 2(1 - d/b) \,, \quad \mathtt{g}_2^T \, \mathtt{g}_3 = 2(1 - b/d) \,. \tag{74}$$

We now have all the ingredients to build a source that couples only to the SPPs that propagate in a given direction. Assume that the pair $(\omega, q)$ is on the dispersion curve for the 2-nd mode, in other words, satisfy the equation $s_0(\omega) = \lambda_2(\omega, q)$. Then we can apply the theory of Sec. 6.2. In particular, we have

$$\mathtt{d}_+ = \mathtt{f}_2 \, \mathtt{g}_2^T \, \mathtt{e} \,, \quad \mathtt{d}_- = \mathtt{g}_2 \, \mathtt{f}_2^T \, \mathtt{e} \,, \tag{75}$$

where all quantities should evaluated at the selected dispersion point $(\omega, q)$. If we choose $\mathtt{e} = \mathtt{f}_3$, we will have $\mathtt{d}_+ = 0$ and $\mathtt{d}_- = 2(1 - d/b)\mathtt{g}_2 \neq 0$. If we choose $\mathtt{e} = \mathtt{g}_3$, then $\mathtt{d}_- = 0$ and $\mathtt{d}_+ = 2(1 - b/d)\mathtt{f}_2 \neq 0$. Therefore, by using the right phase relations for the incident field, we can send the wave in either direction.

### 7.2 Numerical example

To illustrate the effect numerically, we take the lattice period of the chain shown in Fig. 2 to be $h = 25.3$nm and the spheroid semi-axes $a_x = a_z = 6.325$nm and $a_y = 42.166...$nm, so that the proportions are $a_x = a_z = 0.25h = 0.15a_y$. The transverse width of the waveguide is $H = 2h = 50.6$nm and the shift of the central dipole is $\delta = 0.25h = 6.325$nm. Particles are made of a Drude metal with $\epsilon_0 = 5.0$ and the wavelength at the plasma frequency in vacuum $\lambda_p = 2\pi c/\omega_p = 136.1$nm, which is characteristic of silver. The host medium is assumed to be a transparent dielectric with $\epsilon_h = 2.5$. These parameters and the geometry shown in Fig. 2 characterize the waveguide completely.

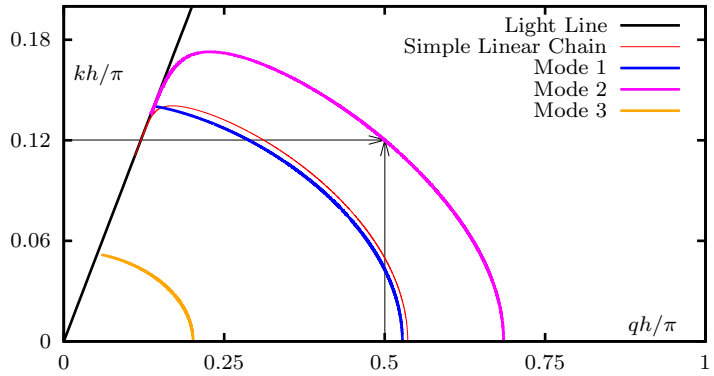


**Fig. 3** Dispersion curves for the chain shown in Fig. 2 with the parameters described in the text. The thin red curve for a simple linear chain of the same spheroids and with the same period is shown for comparison.

We have solved the dispersion equations $s_0(\omega) = \lambda_i(\omega, q)$ by the method of bisection. The dispersion curves for all three modes of the waveguide are shown in Fig. 3. The $i = 1$ mode does not involve the central dipole (which is identically zero for this mode) and therefore it is not very different from the mode of a simple linear chain made of the same spheroids. The dispersion curve for the latter case is shown by a thin red line for comparison. As the eigenvectors $\mathtt{f}_1 = \mathtt{g}_1$ are orthogonal to all other eigenvectors, the $i = 1$ mode cannot be used for direction-selective coupling. However, we can use to this end the $i = 2$ and $i = 3$ modes. Without loss of generality, we choose $i = 2$. The point $(kh/\pi, qh/\pi) = (0.12, 0.5)$ belongs to the $i = 2$ dispersion curve as is shown by the arrows in Fig. 3. Note that, at the normalized frequency $kh/\pi = 0.12$, there exist two solutions to the dispersion equation, one with $i = 1$ and another with $i = 2$. However, the $i = 1$ mode is antisymmetric and will not be excited. We can therefore focus on the $i = 2$ mode alone.

Having fixed a point on the dispersion curve $(kh/\pi, qh/\pi) = (0.12, 0.5)$, we have used numerical summation to compute the matrix elements $w_{11} = a$, $w_{12} = b$,

$w_{13} = c$, and $w_{21} = d$. We then used (72) to find the eigenvectors. In this manner, we arrived at the numerical result

$$\begin{aligned} \mathtt{f}_3 &= \begin{bmatrix} 1 & -(1.37131 + 0.471286\,\mathrm{i}) & 1 \end{bmatrix}^T , \\ \mathtt{g}_3 &= \begin{bmatrix} 1 & -(1.37131 - 0.471286\,\mathrm{i}) & 1 \end{bmatrix}^T . \end{aligned} \tag{76}$$

The theory predicts that, if we use $\mathtt{e} = \mathtt{f}_3$ or $\mathtt{e} = \mathtt{g}_3$ at the normalized frequency $kh/\pi = 0.12$, the resulting SPPs will propagate only in one direction from the excitation site. We show that this is indeed the case by finding the solution to the coupled-dipole equation (2) directly. We have solved the equations in a chain consisting of 8,000 unit cells with the small relaxation constant $\gamma/\omega_p = 0.0005$ (smaller than in realistic metals). Only three dipoles in the central (reference) cell were illuminated, and the incident field amplitudes were given either by $\mathtt{f}_3$ or by $\mathtt{g}_3$ whose components are listed in (76).

The results are shown in Fig. 4. When interpreting Fig. 4, it should be kept in mind that dispersion at $kh/\pi = 0.12$ is negative. Therefore, when we take $\mathtt{e} = \mathtt{g}_3$, we have $\mathtt{d}_- = 0$ and $\mathtt{d}_+ \neq 0$ but the excitation propagates to the left (in the negative $Z$ direction). In any event, we have demonstrated that, by changing the phase relations of the localized source, we can send the excitation either to the right or to the left, with a high efficiency. We note that the quantities shown in the figure are linear in dipole moments; the energy-related quantities are quadratic. Therefore the ratio of energy propagating to the left and right in any of the two excitation schemes illustrated in the figure is of the order of $10^4$, which quantifies the directionality of excitation.

## 8 Discussion

Several aspects of the above numerical demonstration require additional discussion. First, we have used an unrealistically small value of the Drude relaxation constant, $\gamma/\omega_p = 0.0005$. This was done to demonstrate the accuracy of the quasi-particle pole approximation. In Fig. 5 we show the same computation with $\gamma/\omega_p = 0.002$, which is the characteristic value for silver. It can be seen that in this, more realistic case, the SPP can still propagate unidirectionally over 100 unit cells (about 2.5$\mu$m for the parameters used in the simulation) without significant decay of the amplitude.

In the geometry considered above (discrete waveguide made of relatively small particles embedded in infinite free space or a transparent dielectric), the material of the waveguide must be metal. Otherwise, the dispersion relation $s_0(\omega) = \lambda_i(\omega, q)$ does not have real-valued solutions. If we relax the assumptions that the particles are small and the surrounding space is infinite and homogeneous, it may be possible to use other materials such as transparent dielectrics. Familiar examples include optical fibers and dielectric slab waveguides. In the conventional implementation, these waveguides are not directional and therefore do not allow direction-selective coupling. However, we can give the dielectric waveguides a sense of direction by

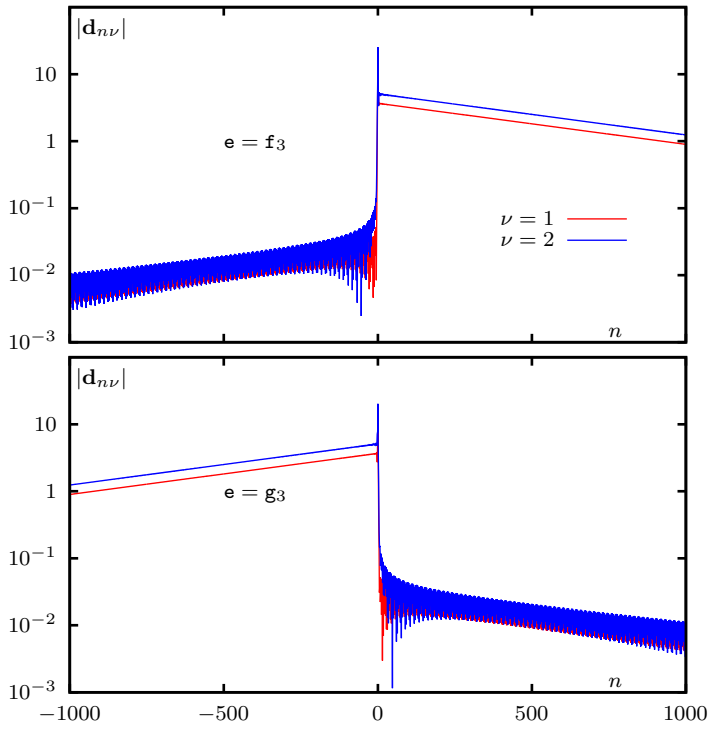


**Fig. 4** Unidirectional propagation of SPPs in the chain shown in Fig. 2 at the dimensionless frequency $kh/\pi = 0.12$ and for the Drude relaxation constant $\gamma/\omega_p = 0.0005$. Only three dipoles in the reference cell $n = 0$ are illuminated either with the amplitudes $\mathtt{e} = \mathtt{f}_3$ or $\mathtt{e} = \mathtt{g}_3$, as labeled. Only the central part of the chain consisting of 8, 000 cells is shown. Dipole moments for $\nu = 3$ are identical to those with $\nu = 1$ and are not shown.

corrugating them (i.e., by introducing voids) so that the inversion symmetry is lost. It is therefore possible to reproduce the effect described above in waveguides with very low losses, although numerical demonstration of this possibility is much harder as the dipole approximation is no longer applicable to such waveguides.

In the metallic discrete waveguides described above, low losses may in fact be problematic. If the SPP reaches the physical end of the chain without significant decay, it may be reflected. Transient pulses can traverse the chain several times reflecting back and forth from the chain ends creating noise. In Fig. 6, we show that the problem can be ameliorated by introducing absorbing traps at the physical ends of the chain. One may think of these traps as detectors. The simulation of Fig. 6 was performed in a very long chain with zero absorption ($\gamma = 0$) everywhere except at the chain ends where it increases exponentially from 0 to $0.05\omega_p$ over the length of 100 cells. It can be seen that reflections in this case are completely suppressed.

Finally, it may seem that the excitation scheme used above where the source antenna illuminates only particles in the reference cell is artificial. A real antenna

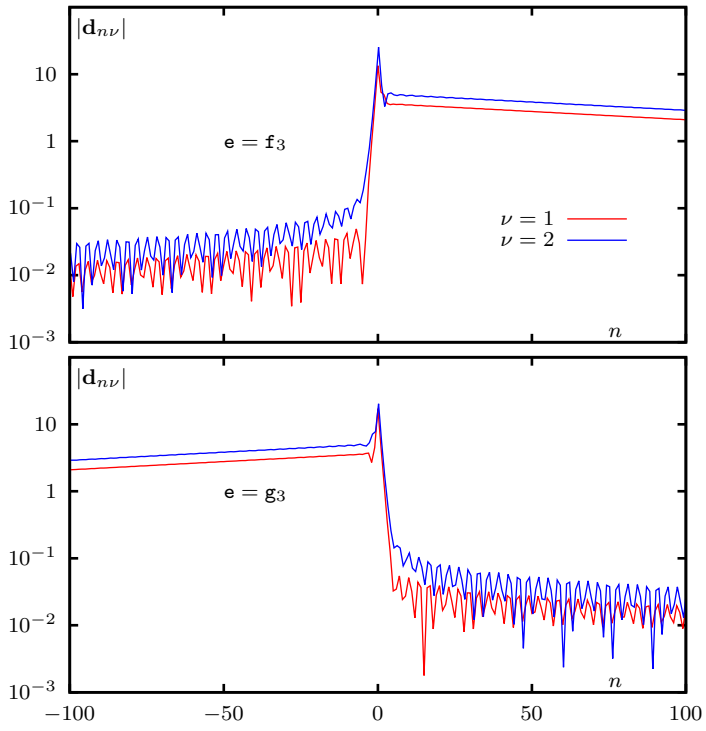


**Fig. 5** Same as in Fig. 4 but for $\gamma/\omega_p = 0.002$.

would illuminate all particles in the chain, albeit with a variable amplitude. The excitation scheme however is physical and in fact quite natural as we will now explain. Let us assume that the external fields $\mathbf{e}_{n\nu}$ in (2) are localized according to (57) and therefore are zero for all $n \neq 0$. We can iterate (2) once by writing

$$\mathbf{d}_{n\nu} = \alpha_\nu(\omega)\mathbf{e}_{n\nu} + \mathbf{d}'_{n\nu} \,. \tag{77}$$

In the adopted excitation scheme, we have $\mathbf{d}_{n\nu} = \mathbf{d}'_{n\nu}$ for all $n \neq 0$, the difference being limited to the reference cell. By substituting (77) into (2), we find that the dipole moments $\mathbf{d}'_{n\nu}$ satisfy

$$\hat{\chi}_\nu(\omega)\,\mathbf{d}'_{n\nu} = \mathbf{e}'_{n\nu} + \sum_{\substack{m\mu \\ (m\mu)\neq(n\nu)}} \hat{G}(\mathbf{r}_{n\nu}, \mathbf{r}_{m\mu};\, \omega)\,\mathbf{d}'_{m\mu} \,, \tag{78}$$

where

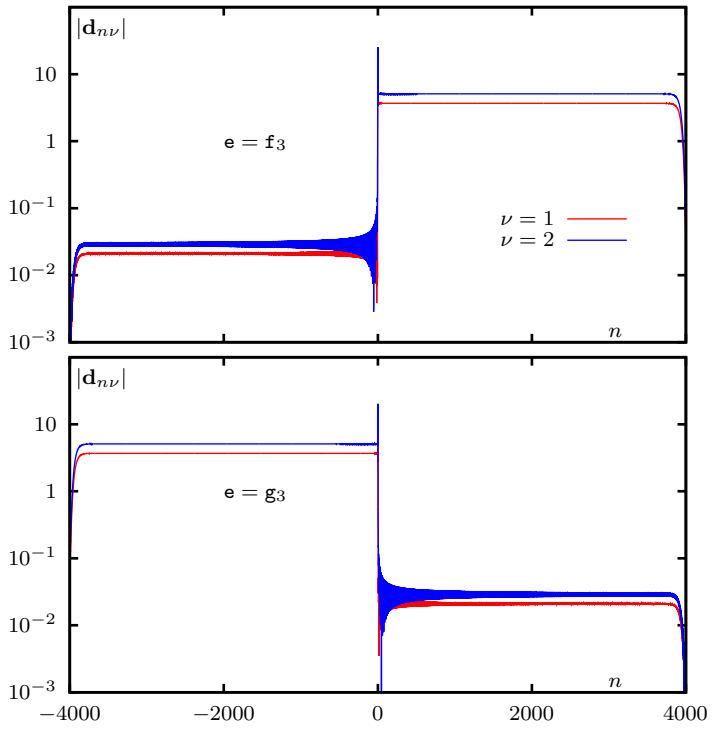


**Fig. 6** Unidirectional SPPs in a chain of 8,000 unit cells made mostly of nonabsorbing particles but with absorbing traps at both ends. The Drude relaxation constant increases exponentially near the chain ends as $\gamma_0 \exp(-\beta m)$ where $\gamma_0/\omega_p = 0.05, \beta = 0.01$ and $m$ is the distance to the chain end in units of $h$. The traps prevent SPP reflections that would occur otherwise.

$$\mathbf{e}'_{n\nu} = \sum_{\substack{\mu=1 \\ (0\mu)\neq(n\nu)}}^{p} \hat{G}(\mathbf{r}_{n\nu}, \mathbf{r}_{0\mu};\, \omega)\, \hat{\alpha}_\mu(\omega)\mathbf{e}_\mu \,. \tag{79}$$

Equation (78) is similar to (2) but has a different source term, $\mathbf{e}'_{n\nu}$. This modified term is the field of an antenna consisting of the particles of the reference cell whose active (that is, externally-controlled) dipole moments are $\mathbf{d}_\nu^{(\text{source})} = \hat{\alpha}_\nu(\omega)\mathbf{e}_\nu$. Thus, for all dipoles except those of the reference cell, the localized excitation scheme considered above is equivalent to the excitation scheme in which the particles of the reference cell are themselves an active source of radiation (the antenna). This alternative excitation scheme is illustrated in Fig. 7. We conclude that the direction-selective coupling can be achieved if the reference cell (located arbitrarily inside a chain) is an externally-controlled active antenna.

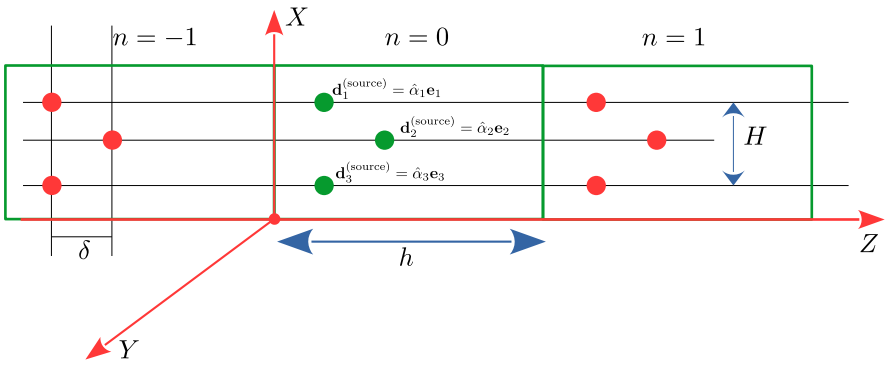


**Fig. 7** Discrete waveguide similar to that of Fig. 2 but here the particles of the reference cell comprise an active antenna (the source of electromagnetic field) and have the externally controlled dipole moments $\mathbf{d}_\nu^{(\mathrm{source})}$. This excitation scheme is equivalent to the localized excitation scheme considered elsewhere in this chapter for all cells wth $n \neq 0$ provided that $\mathbf{d}_\nu^{(\mathrm{source})} = \hat{\alpha}_\nu(\omega)\mathbf{e}_\nu$. The relation must hold at the working frequency for a monochromatic excitation or point-wise in Fourier domain for transient excitation.

## Appendix

The Green's tensor for Maxwell's equations is singular. The singular part appears implicitly in the definition of the polarizability tensor $\hat{\alpha}_\nu(\omega)$ but not in the coupled-dipole equation (2) or the definitions of the dipole sum (8). We therefore focus on the regular part of the Green's tensor, which gives the correct expression as long as $\mathbf{r} \neq \mathbf{r}'$. In terms of the scaled coordinates, the dimensionless Green's tensor appearing in (2) is given by

$$\hat{G}(\mathbf{r},\mathbf{r}';\omega) = \left[\left(\frac{\omega^2}{\rho} + \frac{\mathrm{i}\,\omega}{\rho^2} - \frac{1}{\rho^3}\right)\hat{I} + \left(-\frac{\omega^2}{\rho} - \frac{3\mathrm{i}\,\omega}{\rho^2} + \frac{3}{\rho^3}\right)\frac{\boldsymbol{\rho}\otimes\boldsymbol{\rho}}{\rho^2}\right] e^{\mathrm{i}\,\omega\rho}\,, \tag{80}$$

where

$$\boldsymbol{\rho} = \mathbf{r} - \mathbf{r}' = \frac{\mathbf{r}-\mathbf{r}'}{h}\,, \tag{81}$$

the symbol $\otimes$ denotes tensor product, and $\hat{I}$ is the identity tensor.

Let $\alpha, \beta = x, y, z$ label the Cartesian components of vectors in a rectangular frame. Then we can re-write the above expression in components as

$$G_{\alpha\beta}(\mathbf{r},\mathbf{r}';\omega) = \left[\left(\frac{\omega^2}{\rho} + \frac{\mathrm{i}\,\omega}{\rho^2} - \frac{1}{\rho^3}\right)\delta_{\alpha\beta} + \left(-\frac{\omega^2}{\rho} - \frac{3\mathrm{i}\,\omega}{\rho^2} + \frac{3}{\rho^3}\right)\frac{\rho_\alpha\rho_\beta}{\rho^2}\right] e^{\mathrm{i}\,\omega\rho}\,, \tag{82}$$

Here $\rho^2 = \sum_\alpha \rho_\alpha^2 = \rho_x^2 + \rho_y^2 + \rho_z^2$.

## References


1. S. Zou, N. Janel, G.C. Schatz, J. Chem. Phys. **120**(23), 10871 (2004)
2. V.G. Kravets, F. Schedin, A.N. Grigorenko, Phys. Rev. Lett. **101**, 087403 (2008)
3. V.G. Kravets, F. Schedin, A.V. Kabashin, *et al.*, Opt. Lett. **35**, 956 (2010)
4. B.D. Thackray, P.A. Thomas, G.H. Auton, F.J. Rodriguez, O.P. Marshall, V.G. Kravets, A.N. Grigorenko, Nano Lett. **15**, 3519 (2015)
5. M.L. Brongersma, J.W. Hartman, H.A. Atwater, Phys. Rev. B **62**(24), R16356 (2000)
6. D.S. Citrin, Opt. Lett. **31**(1), 98 (2006)
7. K.B. Crozier, E. Togan, E. Simsek, T. Yang, Opt. Expr. **15**(26), 17482 (2007)
8. P.J. Compaijen, V.A. Malyshev, J. Knoester, Opt. Expr. **23**(3), 2280 (2015)
9. V.A. Markel, J. Mod. Opt. **40**(11), 2281 (1993)
10. V.A. Markel, J. Phys. B **38**, L115 (2005)
11. V.A. Markel, A.K. Sarychev, Phys. Rev. B **75**, 085426 (2007)
12. A.A. Govyadinov, V.A. Markel, Phys. Rev. B **78**(3), 035403 (2008)
13. A.B. Evlyukhin, C. Reinhardt, U. Zywietz, B.N. Chichkov, Phys. Rev. B **85**, 245411 (2012)
14. S.D. Swiecicki, J.E. Sipe, Phys. Rev. B **95**, 195406 (2017)
15. V.E. Babicheva, A.B. Evlyukhin, Phys. Rev. B **99**, 1954444 (2019)
16. A. Poddubny, A. Miroshnichenko, A. Slobozhanyuk, Y. Kivshar, ACS Phtonics **1**, 101 (2014)
17. Y.L. Zhang, R.P.H. Wu, A. Kumar, T. Si, K.H. Fung, Phys. Rev. B **97**, 144203 (2018)
18. V.G. Kravets, A.V. Kabashin, W.L. Barnes, A.N. Grigorenko, Chem. Rev. **118**, 5912 (2018)
19. A.D. Utyushev, V.I. Zakomirnyi, I.L. Rasskazov, Reviews in Physics **6**, 100051 (2021)
20. V.A. Markel, J. Quant. Spectrosc. Radiat. Transfer **236**, 106611 (2019)